STM JOURNALS

Dynamic Integration and Control of Fixed-Speed Wind Generation System with Multimachine System

A. H. M. A. Rahim*, S. A. Al-Baiyat

Department of Electrical Engineering, King Fahd University of Petroleum & Minerals, Dhahran-31261, Saudi Arabia

ABSTRACT

Since the average life of a wind generator is about 20 years, many of the wind systems will be employing conventional fixed-speed cage generators in spite of the superiority of the variable-speed devices. As the extent of wind integration continues to grow, the wind parks may need to be integrated with AC power grids. The integration to grids, particularly to weak ones, may give rise to transient conditions detrimental to both the asynchronous as well as synchronous systems. This article presents an integrated dynamic model of the fixed-speed wind system with a multimachine AC power system. Simulation studies of a 4-machine 12-bus system indicate that under some contingencies a small steady slip may continue to pump transients harmful for both the systems. A frequency controller in the electro-mechanical loop of the wind system has been shown to mitigate the problem effectively.

Keywords: Wind system modeling simulation, induction generator control, multimachine power system, dynamic study

*Author for correspondence E-mail**:** ahrahim@kfupm.edu.sa

INTRODUCTION

In the early stages of wind power development, most wind farms were equipped with fixed-speed cage-type wind generators. The power efficiency of such fixed-speed devices is fairly low for most wind speeds and they are being replaced by variable-speed operation. Since the life expectancy of these machines is about 20 years, many of the existing devices will continue for a good period of time. Wind power penetration levels have increased in electricity supply systems in a number of countries in recent years; so have increased concerns about how to incorporate this significant amount of intermittent, uncontrolled and non-dispatchable generation without disrupting the finely-tuned balance that network systems demand. Measures such as aggregation of wind turbines, load and wind

forecasting and simulation studies are expected to facilitate larger grid penetration of wind power [1].

Increasing wind power penetration in a power system means that wind turbines substitute the conventional power plants that traditionally control and stabilize the power system. If wind power penetration exceeds a certain level, wind turbines have to be involved in performing these control tasks since it has been recognized that wind turbines themselves have an influence on the dynamic behavior of the power system, which they are connected to. A stable power system is also of great importance for wind turbines, as variations in grid voltage and frequency have considerable impacts on the operation of wind turbines [2]. Assessment of the effect of the wind power penetration to an existing power system

necessitates the calculation of voltage and frequency profiles and examination of instability issues. While the steady state and transient performance of wind turbine generators connected to infinite bus AC systems are well documented [35], details of dynamic integration procedures are rather limited.

The studies reported for multimachine asynchronous-synchronous machines often use various types of commercial power system dynamic simulation packages like PSS/E [6], PSCAD/EMTDC [7], DigSilent [8], Mudapack [9], etc. These softwares employ both eigenvalue-based frequency domain as well as time-domain analyses. Some studies through frequency domain analysis seem to give more insight about the system behavior [10]. The asynchronous generators are considered to be devices that inject real power drawing reactive power, which may not adequately represent the dynamic impact on the power system.

In an autonomous grid supplied by asynchronous wind turbine system, the voltage and frequency fluctuations will be considerably greater than in a normal synchronous AC system. Hence, the nonlinearities of the system equations must be included in the transient stability representation. Models of the wind turbine, induction generator, synchronous generator, automatic voltage regulator, compensating capacitor banks, the transmission network, the load, etc., have to be properly represented for accurate analysis [11, 12]. These models normally are written in their individual reference frames. Precision analyses demand that the network quantities should be appropriately transformed for integrated system study.

This article presents a detailed model of a fixed-speed induction generator system which integrates the dynamics of multimachine synchronous system through an angle-dependent transformation technique. The transient behavior of the integrated multimachine system indicates undesirable transient phenomenon for some contingencies. A procedure to remedy the situation through a frequency controller has been explored.

COMPONENT MODELS

Figure1 shows the schematic of an AC power system having an infeed from an asynchronous wind-generator system. The wind-generator system comprises of a horizontal-axis wind turbine and a fixed-speed induction generator, which connects to the multimachine AC system over its transmission network. The local load and power factor correcting capacitors are connected to the generator terminal. The models of the individual components are briefly presented in Figure 1 [13].
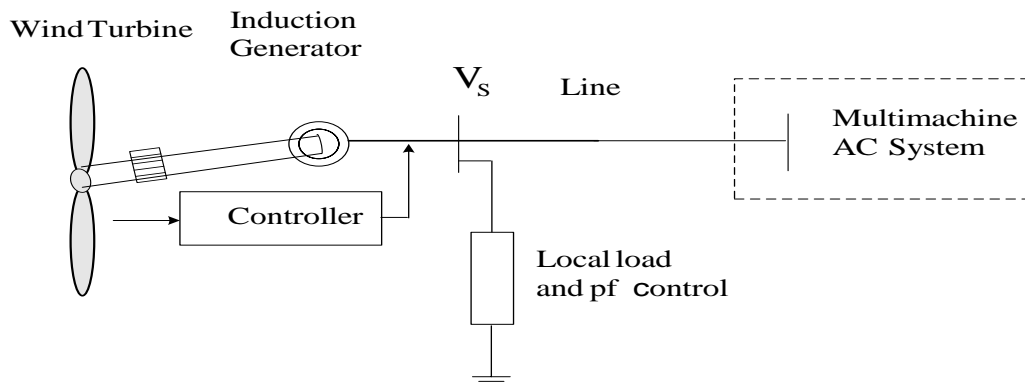
STM JOURNALS

Fig.1 Wind Turbine-Generator System Connected to the AC System.

Wind Turbine System

The mechanical power output of a wind turbine is related to the wind speed V_w by

$$P_m = \frac{1}{2}\rho A . C_p(\lambda, \beta).V_w^3 \qquad (1)$$

Here, ρ is the air density and A is the swept area by the turbine blades. The power coefficient $C_p(\lambda, \beta)$ depends on both blade pitch angle β and tip speed ratio defined as,

$$\lambda = \frac{\Omega R}{V_w} \qquad (2)$$

where, R is wind turbine rotor radius and Ω is the mechanical angular velocity. Expression for C_p is given by [14],

$$C_p(\lambda, \beta) = 0.5176\left(\frac{116}{\lambda_i} - 0.4\beta - 5\right)e^{\frac{-21}{\lambda_i}} + 0.0068\lambda$$

$$\frac{1}{\lambda_i} = \frac{1}{\lambda + 0.08\beta} - \frac{0.035}{\beta^3 + 1} \qquad (3)$$

Some typical plots of mechanical power (P_m) for various wind speeds, and for zero blade pitch angle *(β)*, are shown in Figure 2.
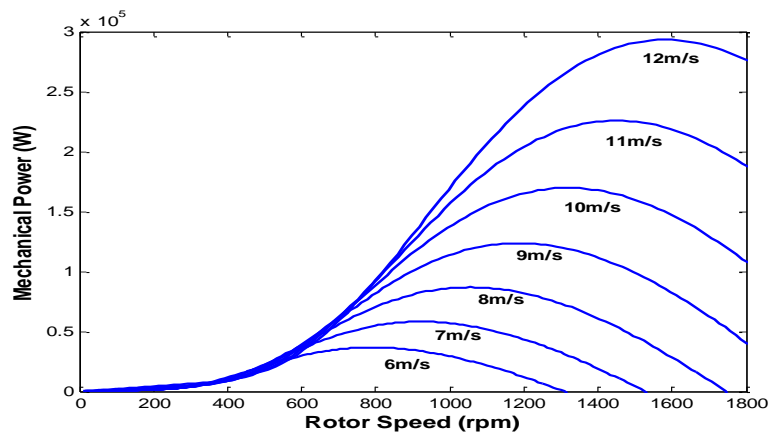

Fig. 2 Speed versus Power Output Characteristics of a Wind Turbine.

Induction Generator

A 4th order dynamic model for the cage induction machine can be arrived at from the voltage-current-flux relationship of Krause [15]. Induction generator rotor circuit voltage-current-flux relations can be expressed in terms of internal voltages e_d' and e_q' behind transient impedance $R_s + jx'$ [16]. The dynamic relationships for the stator and rotor circuits are written as,

$$\dot{i}_{ds} = \frac{\omega_0}{x'}\left[-\left(R_s + R_r\left(\frac{x_m}{x_{rr}}\right)^2 \right)i_{ds} + x'i_{qs} + (1-s)e_d' - (\frac{R_r}{x_{rr}})e_q' - v_{ds} + (\frac{x_m}{x_{rr}})v_{dr} \right]$$

$$\dot{i}_{qs} = \frac{\omega_0}{x'}\left[-\left(R_s + R_r\left(\frac{x_m}{x_{rr}}\right)^2 \right)i_{qs} - x'i_{ds} + (1-s)e_q' + (\frac{R_r}{x_{rr}})e_d' - v_{qs} + (\frac{x_m}{x_{rr}})v_{qr} \right]$$

(4)

$$\dot{e}_d' = \omega_0\left[-(\frac{R_r}{x_{rr}})e_d' + se_q' + R_r\left(\frac{x_m}{x_{rr}}\right)^2 i_{qs} - (\frac{x_m}{x_{rr}})v_{qr} \right]$$

$$\dot{e}_q' = \omega_0\left[-(\frac{R_r}{x_{rr}})e_q' - se_d' - R_r\left(\frac{x_m}{x_{rr}}\right)^2 i_{ds} + (\frac{x_m}{x_{rr}})v_{dr} \right]$$

(5)

In the above,

$$s = \frac{\omega_0 - \omega_R}{\omega_0} \qquad x' = x_s + \frac{x_m x_r}{x_m + x_r} \; ; \qquad T_o' = \frac{x_m + x_r}{\omega_b R_r}$$

(6)

$$e_d' = -\frac{x_m}{x_m + x_r}\psi_{qr} \; ; \qquad e_q' = \frac{x_m}{x_m + x_r}\psi_{dr}$$

(7)

A list of symbols is given under Nomenclature. If stator transients are not included, the differential relationship Eq. (4) will be replaced by algebraic equations,

$$v_{ds} = -R_s i_{ds} + x'i_{qs} + e_d'$$
$$v_{qs} = -R_s i_{qs} - x'i_{ds} + e_q'$$

(8)

The slip equation for the turbine-generator equivalent mass is,

$$\Delta s = \frac{1}{2H}[P_m - P_e - D\Delta s]$$

(9)

Here, the electrical power output P_e can be approximated as,

$$P_e = e_d'i_{ds} + e_q'i_{qs}$$

(10)

Synchronous Generator

Neglecting the stator transients, each synchronous generator in the power system is represented through a 5th order model [17],

$$\dot{e}'_q = \frac{1}{T'_{do}}\left[E_{fd} - e'_q - (x_d - x'_d)i_{ds} \right]$$

$$\dot{e}'_d = \frac{1}{T'_{qo}}\left[-e'_d + (x_q - x'_q)i_{qs} \right]$$

$$\dot{\omega} = \frac{1}{2H}\left[P_m - P_e - P_D \right] \qquad (11)$$

$$\dot{\delta} = \omega_0 \Delta\omega$$

$$\dot{E}_{fd} = \frac{1}{T_A}\left[K_A(V_{ref} - V_t) - E_{fd} \right]$$

In the above,

$$P_e = e'_d i_{ds} + e'_q i_{qs} + (x'_q - x'_d)i_{ds}i_{qs}; \quad P_D = D\Delta\omega$$

The state variables are the generator internal voltages along d-q axes, angular frequency, rotor angular position and the field voltage, respectively. Similar to the induction generator, the stator voltage and currents of the synchronous generator are related through,

$$\begin{aligned} v_{ds} &= -r_s i_{ds} + x'_q i_{qs} + e'_d \\ v_{qs} &= -r_s i_{qs} - x'_d i_{ds} + e'_q \end{aligned} \qquad (12)$$

INTEGRATED SYSTEM MODEL

The models for the different components in the multimachine power system are generally written in their own frames of reference. In the simplest but common case the whole load or part of this can be modeled as impedance $Z_L = R_L + j\omega L_L$. When the active load P_L and reactive load Q_L are known at steady state, the values of resistance and reactance can be obtained from the relation,

$$P_L + jQ_L = |V_t|^2 Y_L^* \qquad (13)$$

Y_L^* denotes the conjugate of load admittance.

The transmission network is considered to be in quasi-static state whose voltage current phasors are considered to be rotating at synchronous speed and written in network (D-Q) frames of reference. The network admittance matrix can be reduced to obtain Y_{red} with dimension $2N \times 2N$, where N is the number of generator buses. The injected currents from the generator buses in (D-Q) network frame of reference are then written as,

$$I_{DQ} = Y_{red}V_{DQ} \qquad (14)$$

The synchronous generator quantities written in their individual (d-q) frames are related to the network frame D-Q through [17],

$$[F]_{DQ} = [T][F]_{dq} \qquad (15)$$

where, F may be either V or I. The transformation matrix T is written as,

$$T = dig[e^{j(\delta-\pi/2)}] = dig[rot(\delta_1), rot(\delta_2),....., rot(\delta_G)] \qquad (16)$$

Here,

$$rot(\delta) = \begin{bmatrix} \sin\delta & \cos\delta \\ -\cos\delta & \sin\delta \end{bmatrix}$$

The rotor angle δ of a synchronous machine is considered to be aligned with voltage behind quadrature axis synchronous reactance. The induction generator equations are normally written in terms of synchronously rotating arbitrary (d-q) frames which are considered to be fixed with respect to the network D-Q frame. These fixed quantities can be integrated with the general relationship Eq. (15) through the assumption of induction generator angle δ_{ig} written as [18],

$$\delta_{ig} = \pi/2 + \angle V_{ig} \qquad (17)$$

where, phasor V_{ig} refers to the terminal voltage of the induction generator. Induction generator d-axis is considered to be aligned with its terminal voltage. Using Eqs. (14) and (16), the relationship of injected current and resultant node voltages can be written along the machine reference frames as,

$$I_{dq} = T^{-1}Y_{red}TV_{dq} \qquad (18)$$

From Eqs. (8) and (12), the stator currents for both the induction and synchronous generators is written in the form,

$$V_{dq} = [Z]I_{dq} + E'_{dq} \qquad (19)$$

Substituting Eq. (18) in Eq. (19), the non-state currents can be expressed in terms of the state variables as,

$$I_{dq} = [1-Y_mZ]^{-1}Y_mE'_{dq}; \quad Y_m = T^{-1}Y_{red}T \qquad (20)$$

These are then substituted back in the original relationships to give a closed-form state representation.

For inclusion of turbine output power P_m in the closed-form dynamic representation, Eq. (1) is expressed through an analytical expression in terms of induction generator rotor speed (ω_R). The turbine output power is plotted for a specific wind speed V_w and then a curve-fitting method is employed to generate a relationship of the form,

$$P_m = a_p\omega_R{}^p + a_{p-1}\omega_R{}^{p-1} + a_{p-2}\omega_R{}^{p-2} + \ldots\ldots\ldots + a_0 \qquad (21)$$

The complete dynamic model of the multimachine is obtained by combining differential relationships in Eqs. (4), (5), (9), and (11) along with other algebraic relationships.

INDUCTION GENERATOR SPEED REGULATOR

Asynchronous generators need to be equipped with mechanical and/or electro-mechanical devices for automatically controlling the speed so as to relate the input and output of the

_____

generator [11]. For a constant setting of the speed changer, the static increase in generator output is directly proportional to static frequency drop. After the primary control function, which brings the system to an equilibrium state with a permanent frequency

error, a secondary control is needed which eventually establishes nominal rotational speed by eliminating the static frequency error. The device which performs this action is the

at bus #4. It is assumed that 68 MW is being supplied by the wind farm which has 50 generators each with a capacity of 2 MW. This is approximately 26% of total system

generation considered in this study. The system data is given in the **Appendix**. Typically, in steady state load flow analysis the induction generator is represented as a PQ bus [19, 20]. However, in this work it was considered to be a PV bus having the provision of an additional excitation capacitor at the generator terminal. The capacitance at the bus can be adjusted so that the induction generator system operates almost under unity power factor condition [21]. The slip of the machine is established from the static steady-state model of the induction generator and the corresponding reactive power absorbed by the generator is calculated.
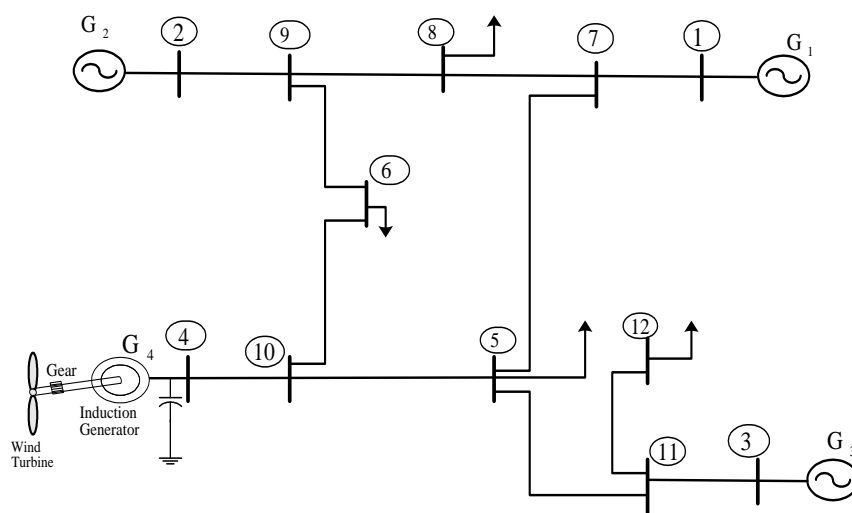

Fig. 4 Multimachine Synchronous System with Wind Input.

The transient behavior of the system was investigated for various contingencies considering two modeling scenarios. These are,

(1) The fixed-speed induction generator connected to the multimachine system without a frequency controller (symbol "No FC" in the figures)

_____

(2) The generator with auxiliary frequency controller (symbol "With FC")

Figures 5–8 show the induction generator transient response for a short wind gust amounting to 50% input torque for 0.2 s. This small disturbance is introduced to study the nature of transients which may arise in the integrated asynchronous-synchronous system. The variation of the machine slip following the disturbance, in Figure 5, shows that the system is slightly oscillatory with strategy (1). The gust causes a relatively large slip error which decays extremely slowly. The corresponding plots for the magnitude of power output and generator terminal voltage are shown in Figures 6 and 7, respectively. While the variation of the magnitude of the terminal voltage is quite normal, an interesting phenomenon is observed in the phase angle of the generator terminal voltage plotted in Figure 8. It can be seen that the phase angle continues to grow in a cyclic manner. For nominal AC system frequency of f_o, the period of this cyclic variation can be shown to be

approximately as,

$$T = \frac{1}{|\Delta s| f_0} \qquad (24)$$

Since the phase angle shift phenomenon occurs in current phasors in a similar manner, it is not reflected in power output of the machine in Figure 6.

The phase angle drift of voltage and current of the induction generator can be corrected by using a frequency controller in the mechanical loop of the induction generator system. Responses with the dotted lines in Figures 58 show the variation of slip, power output, and magnitude and phase of terminal voltage, respectively when the frequency controller is installed. It can be seen that the controller eliminates the slip error very fast. The transients in voltage and power variations have been removed in about 2 s. and normal operating conditions are restored.
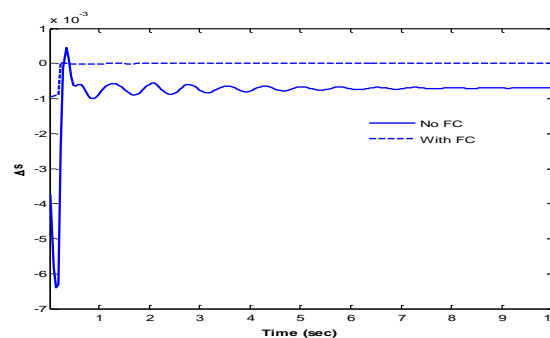

Fig. 5 Change in Slip of Induction Generator Following a Wind Gust Amounting to 50% Input Torque for 0.2 s with (a) No Frequency Controller (No FC), and (b) with Frequency Controller Installed (with FC).
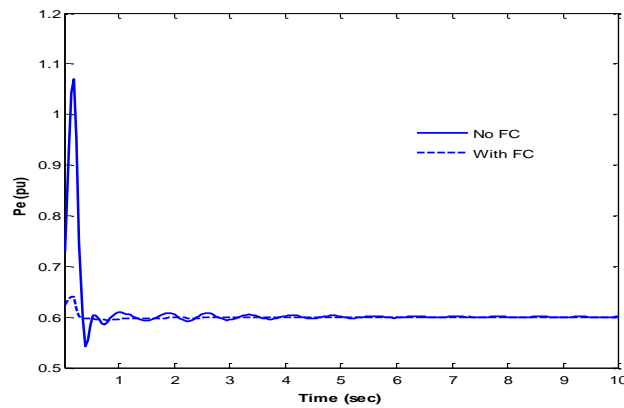
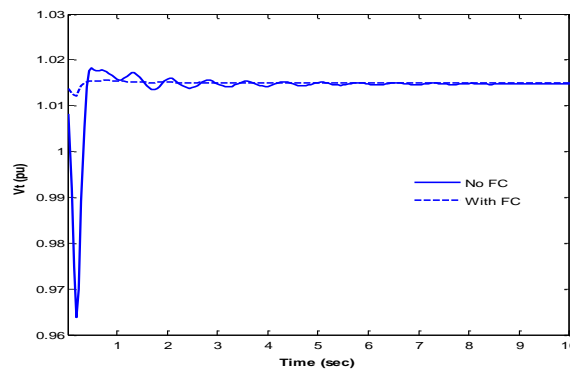**Fig.6** Power Output of Induction Generator Corresponding to Figure 5.

Fig.7 Terminal Voltage Variation of Induction Generator Following the Gust Condition of Figure 5 with (a) No Frequency Controller (No FC) and (b) with Frequency Controller (with FC).
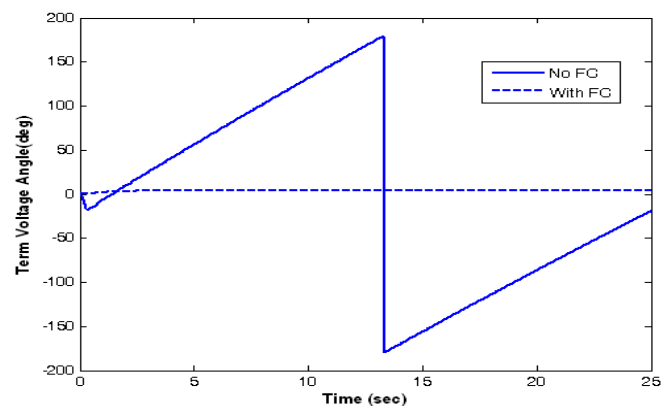

Fig. 8 Phase Angle Variation of Induction Generator Corresponding to Figure 5.

Figure 9 shows the variation of the armature current of synchronous generator located on bus #2. The two responses recorded, with and without frequency controller, show how the transients in the induction generator affect the armature current transients of the synchronous generators.

The wind generator with frequency controller shows a much better transient profile because of the elimination of the variations in induction generator voltage-current phase angles.
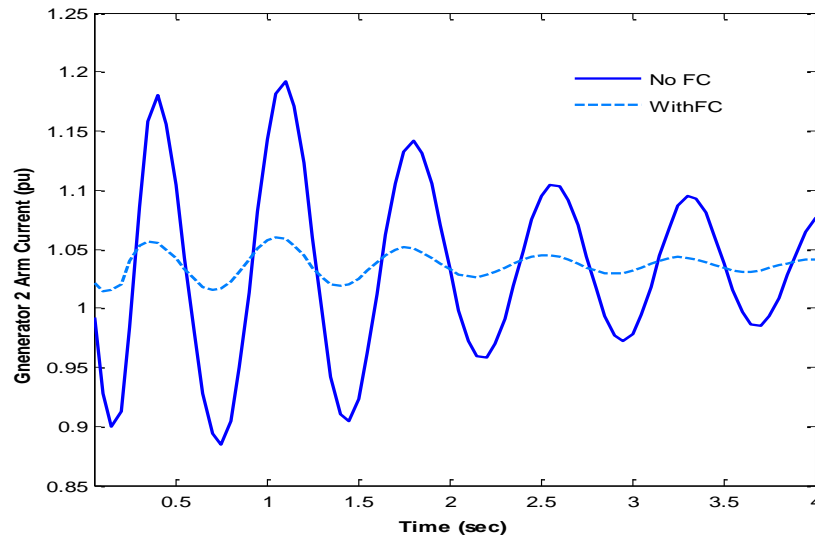

Fig.9 Variation of Armature Current of Synchronous Generator #2 with (a) No Frequency Controller (No FC) and (b) with Frequency Controller (with FC).

The effectiveness of the frequency controller on the induction generator is further verified by considering severe three-phase fault conditions at the point of common coupling (bus #4) in the multimachine system of Figure 4. Three-phase faults of various durations were applied and the transient behavior of the system was examined. It was observed that a three-phase fault for approximately 0.7 s is critical. Any longer fault duration causes a collapse of the generator voltage and the generator slips away to unstable regime as shown in Figure 10. The plots for change in rotor slip are recorded for three cases, (i) for fault duration of 0.7 s without frequency controller, (ii) fault duration of 1 s without frequency controller, and (iii) fault duration of 1 s with frequency controller. In case of (i), there is a steady slip error and the terminal voltage angle phasor rotates at an angular speed of $(\Delta s.f_0)$ as shown by the solid line in Figure 11. Case (ii) represents an unstable situation in the absence of a frequency controller (dotted line, Figure 10). Inclusion of the frequency controller restores the normal operation for the 1 s duration fault

with very little transients (dashed line, Figures 10 and 11). Figure 12 shows the variation of power output for cases (i) and (iii). It is apparent that the frequency controller, in addition to giving better accuracy in terms of dynamic analysis, helps restore normal operation following much larger fault conditio
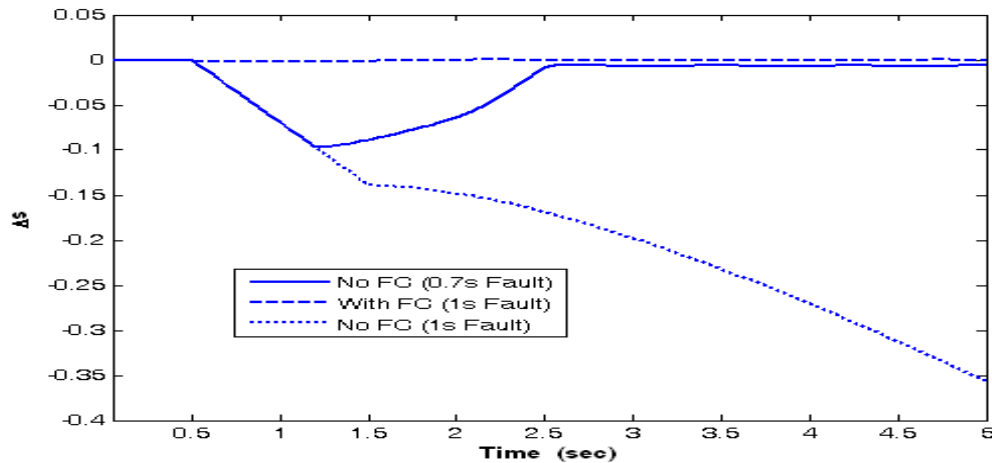

Fig.10 Induction Generator Slip Variation Following Symmetrical Three-Phase Fault at the Point of Common Coupling with (a) 0.7 s Fault Duration, No Frequency Controller, (b) 1 sFault Duration, No Frequency Controller, and (c) 1 s Fault Duration with Frequency Controller (Dashed Line).
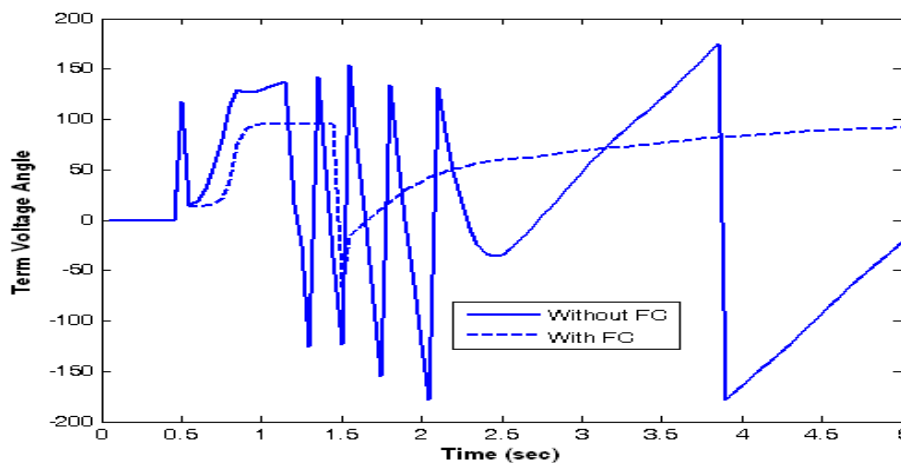

Fig. 11 Phase Angle of Induction Generator Terminal Voltage with (a) 0.7 s Fault Duration, No Frequency Controller (Solid Line) and (b) 1 s Fault Duration with Frequency Controller (Dashed Line).
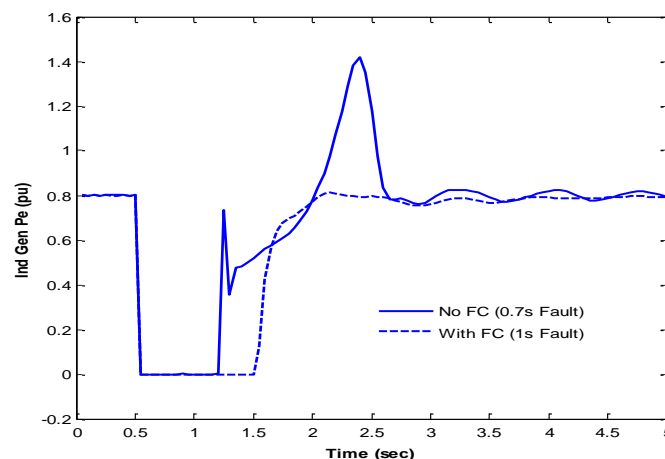
Fig. 12 Induction Generator Power Output with (a) 0.7 s Fault Duration, No Frequency Controller (Solid Line) and (b) 1 s Fault Duration with Frequency Controller (Dashed Line).

CONCLUSIONS

Integration of the dynamics of asynchronous fixed-speed cage-type induction generator with that of synchronous generators in a multimachine AC system is investigated in this article. This study presents a dynamic integration procedure for asynchronous and synchronous generator dynamics with the network variables through an angle-dependent transform. Simulation results obtained through detailed modeling indicate that for certain contingencies, the rotor slip error decays extremely slowly generating unwarranted transients in the system, which is not apparent from normal power flows. This affects the transient performance of both the asynchronous and synchronous machines in the system. It has been demonstrated that the slowly decaying slip error can be eliminated by installing a frequency controller in the electro-mechanical loop of the wind system. The frequency controller damps the system transients effectively and normal operation is restored quickly.

ACKNOWLEDGEMENT

REFERENCES

1. Kumar P. V., Meera K. S. and Kottayil S. K. *International Conference on Power Electronics, Drives and Energy Systems, PEDES '06.* 2006. 16p.
2. Jauch C., Islam S.M., Sorensen, P. et al. *Renewable Energy*. 2007. 32. 23342349p.
3. Nunes V. A., Pecas Lopes, J. A Zürn et

STM JOURNALS

_____

al. *IEEE Transactions on Energy Conversion*. 2004. 692700p.

4. Fernandez R. D., Battaiotto P. E. and Mantz R. J. *Renewable Energy*. 2008. 33. 2258-2265p.

5. Anaya-Lara O., Hughes F. M., Jenkins N. et al. *Wind Engineering*. 2006. 30. 107127p.

6. Slootweg J. G. *Wind Power – Modeling and Impact on Power System Dynamics*. Ph. D. Thesis. Netherlands. Delft Technical University. 2003.

7. Muyeen S. M., Takahashi R., Ali M.H., Murata et al. *IEEE Transactions on Power Systems.* 2008. 23. 11791187p.

8. Jauch C., Sørensen P., Norheim I. et al. *Electric Power Systems Research*. 2007. 77. 135144p.

9. Vowles D. J., Samarasinghe C., Gibbard M. J. et al. *IEEE Power & Energy Society General Meeting*. July 2008. 18p.

10. Mei F. and Pal B. *IEEE Transactions on Energy Conversion*. 2007. 22. 728736p.

11. Stavrakasis G.S. and Kariniotakis G.N. *IEEE Transactions on Energy Conversion*. 1995. 10. 577–583p.

12. Stavrakasis G.S. and Kariniotakis G.N. *IEEE Transactions on Energy Conversion.* 1995. 10. 584–590p.

13. Rahim A.H.M.A. and Nowicki E.P. *Electric Power Systems Research*, 2011. 81. 149–157p.

14. Heier S. *Grid Integration of Wind Energy Conversion Systems*. 2nd Ed. New York. John Wiley & Sons Ltd., 2007.

15. Krause P. *Analysis Electric Machinery and Drive Systems*. IEEE New York. Press & John Wiley. 2002.

16. Kundur P. *EPRI Power System Engineering*. 1994.

17. Anderson P.M. and Fouad A.A. *Power System Control and Stability*. 2nd ed. IEEE Press: Wiley Interscience. 2003.

18. Rahim A.H.M.A. *Proceedings of Waset Conference*, Paris. June 2011.

19. Feijoo, E. and Cidras, J. *IEEE Transactions on Power Systems*. 2000. 15. 110–115p.

20. Jayashri R. and Devi, R.P.K. *Wind Engineering*. 2006. 30. 303–316p.

21. Akhmatov V. *Induction Generators for Wind Power*. London. Multi-Science Publishing Company, Ltd. 2005.

NOMENCLATURE

V_w	Wind speed
d-q	Direct and quadrature axes
R_s, R_r	Stator, rotor resistance
x_s, x_r	Stator, rotor reactance
x_m	Mutual reactance
x_d, x_q	d-q axes synchronous reactance
x	transient reactance
ψ_{ds}, ψ_{qs}	d-q axes stator flux linkage
ψ_{dr}, ψ_{qr}	d-q axes rotor flux linkage
i_{ds}, i_{qs}	d-q axes stator current
i_{dr}, i_{qr}	d-q axes rotor current
v_{ds}, v_{qs}	d-q axes stator voltage
e_d, e_q	d-q axes internal voltages of generator
s	Slip of induction generator
Efd	Generator field voltage
V_{ref}, V_t	Reference and terminal voltage of generator
K_A, T_A	Gain and time constant of exciter
ω, ω_o	System angular frequency, base angular frequency
ω_R, ω_{Ro}	Generator rotor angular speed, operating ω_R
H, D	Inertia constant, damping coefficient of generator

_____

Table I Generation and Load Data.

Bus #	Generation		Load	
	P_g MW	Q_g MVAR	P_L MW	Q_L MVAR
1	37.5	23.94		
2	105	16.107		
3	50	19.603		
4	60	-		
5			77.5	30
6			52.5	25
8			72.5	27
12			48.75	15

Table III Induction Generator Parameters

R_s = 0.04373	Blade swept area, A = 577 m^2
R_r = 0.024	Air density, ρ = 1.225 kg/m^3
x_s = 3.418	Blade radius, R = 13.5 m
x_r = 3.418	Gear-ratio = 1:23
x_m = 3.289	Pitch angle, β = 0
D = 0.00	Mean wind speed, V_w = 9 m/s
H = 3 s	f_0 = 60 Hz

Table II Line Data in 100 MVA Base.

From bus	To bus	R (pu)	X (pu)	B/2 (pu)
1	7	0	0.05	0
2	9	0	0.05	0
4	10	0.08	0.4	0
3	11	0	0.05	0
11	12	0.018	0.1167	0.0175
11	5	0.009	0.10	0.035
5	10	0.009	0.1167	0.035
10	6	0.009	0.135	0.035
6	9	0.009	0.1075	0.035
9	8	0.009	0.11	0.049
8	7	0	0.1333	0.035
7	5	0.009	0.1333	0.035

.

_____